THE JOURNAL OF PHYSICAL CHEMISTRY B LETTERS

2009, *113,* 8453–8457
Published on Web 06/01/2009

Shear-Induced Deformation of Bovine Insulin in Couette Flow

Innocent B. Bekard and Dave E. Dunstan*

Department of Chemical and Biomolecular Engineering, The University of Melbourne, Melbourne, Victoria 3010, Australia

Received: April 16, 2009; Revised Manuscript Received: May 17, 2009

We have applied a uniform, shear-driven flow field (Couette flow) to study the effect of shear on the structure and conformation of aqueous bovine insulin, in situ and in real time, using intrinsic Tyr fluorescence and circular dichroism (CD) spectroscopy. The morphology of post-shear insulin samples was analyzed using atomic force microscopy (AFM). Both fluorescence and CD data show a shear-dependent deformation of bovine insulin in Couette flow. The shear effect is more pronounced with increasing shear rate. AFM images show large aggregates for insulin samples sheared at 200 and 400 s^{-1}, whereas samples sheared at 600 s^{-1} contained fibrillar forms. We hypothesize that helical segments unfold upon extensional strain in the deformation flow field, resulting in unstructured, aggregation-prone insulin molecules. The occurrence of rotational diffusion in the direction of flow facilitates the coalescence of deformed insulin molecules into oligomeric aggregates. The size of the insulin aggregates diminished with increasing shear rate. This shows that the deformation cycle in fast flow fields retards the formation of large aggregates and promotes the ordering of deformed insulin molecules into the more stable fibrillar forms.

Mechanical destabilization of the higher-order structure of a native protein often leads it to misfold and coalesce into insoluble aggregates.[1] Agitated protein solutions have been shown to aggregate more quickly relative to quiescent samples.[2−4] A number of published studies consider hydrodynamic shear stress as the trigger of protein deformation and subsequent aggregation in agitated protein solutions.[5−10] What is perplexing is the mechanism of shear-induced protein deformation upon agitation. It remains to be known whether shear stress directly disrupts native protein molecules (hence, initiating aggregation[8]) or its influence stems from the continuous generation of an air−liquid interface at which protein molecules, by virtue of their amphipathic nature, aggregate.[10] Whatever the case may be, the mechanical effect is purported to proceed via conformational disorder in the native protein, resulting in its deformation and subsequent exposure of hydrophobic regions to the aqueous environment.[9] Deformed protein molecules associate primarily via hydrophobic interactions and precipitate out of solution as amorphous or fibrillar aggregates or both.[2,11] This observation is a major concern, especially in the bioprocessing of protein therapeutics, such as insulin and immunoglobulin G, because their exposure to shear during pumping, centrifugation, filtration, and fractionation[6] makes them aggregation prone.

Intriguingly, accumulating evidence associates the deterioration of vascular microcirculation with the onset of protein conformational disorders, such as Alzheimer's disease.[12,13] The pathological hallmark of this and related conformational disorders is the precipitation of proteinaceous elements into well-structured, insoluble fibrillar aggregates. Alterations in hemodynamic shear stress on arterial walls participate in the pathogenesis of atherosclerosis, which also involves the deposition of proteinaceous material in the form of artheromatous plaque.[14,15] Shear-dependent unfolding of protein components in the three-dimensional structure of human von Willebrand factor has also been reported.[16] Furthermore, in vitro studies on well-defined food and drug protein systems, including β-lactoglobulin and insulin, show that these proteins form large aggregates/fibrils under shear.[9,17] It is thought that shear stress (which can be decomposed into stretch and compressive pressure) resulting from flow is what triggers protein deformation and subsequent aggregation.[6] The key question that remains to be solved is the relationship between shear and the extent of protein deformation and, hence, the mechanism involved in the process. It is noteworthy that understanding the rheological properties of proteins is of critical importance in defining their conformational and structural attributes in flow.

We have previously shown that shear flow induces amyloid fibril formation[7] and more recently explained how shear affects protein aggregation using amyloid-β as a model protein.[18] We observed that shear accelerates the nucleation and polymerization of amyloidogenic oligomers into protofibrils but inhibits their fusion into mature fibrils. We and others have reported that the effect of shear on protein aggregation is only critical at the onset of shear flow and not continuous shear flow itself.[8,18]

Although there has been progress in investigating the influence of shear flow on protein aggregation, little work has been expended on the effect of shear on a protein's secondary or tertiary structure[9] as determined by fluorescence and circular dichroism spectroscopy. Hence, current literature fails to address the relationship between shear and the extent of deformation of the higher-order structure of a native protein, a prerequisite for aggregation.[1,5] Here, we report shear-induced changes in the structure and conformation of aqueous bovine insulin, in situ and in real time, using intrinsic Tyr fluorescence and CD

* Corresponding author. Tel.: +61 (03) 8344 8261. Email: davided@unimelb.edu.au.

10.1021/jp903522e CCC: $40.75

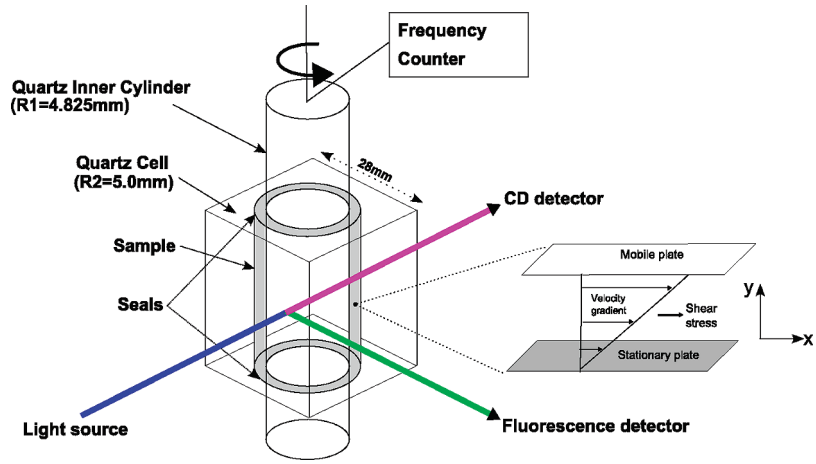

Figure 1. Schematic depicting the shear device and Couette flow profile (inset). The flow is in the *x* direction, whereas the velocity gradient is in the *y* direction.

spectroscopy respectively. The morphology of sheared insulin samples was analyzed using atomic force microscopy. A well-defined, shear-driven flow field (Couette flow) was applied in this work, as opposed to the variable flow fields (generated by stirring and by shaking) employed by others.[2,9] The experiments were conducted at ambient temperature, thus limiting thermal contributions to insulin deformation.

Bovine insulin (Sigma) was chosen as the model protein for this study because (i) it is a well-characterized protein system; (ii) it is economical and easy to use, and (iii) it has been shown to form aggregates under shear. Insulin is a 51-amino-acid peptide hormone produced in commercial quantities and administered as a protein drug in treating insulin-dependent diabetics. Conventional purification of insulin involves exposure of insulin solutions to low pH, extreme temperatures, and shear.[2,19] These conditions are known to promote insulin aggregation and have been an issue of concern in quality control during insulin isolation, transportation, and storage. Fibrillar insulin aggregates have been reported both in patients with type II diabetes, especially after repeated administration of the protein drug,[20] and in normal aging.[21] We studied the influence of simple shear flow on native bovine insulin using a custom-made shear cell with Couette geometry. The shear rates investigated were 200, 400, and 600 s^{-1}, which are within physiological range. Arterial wall shear rates are estimated to range between 134.2 and 1640 s^{-1}.[22] Blood plasma contains both cells and a range of proteins. Blood is generally modeled as a Bingham plastic with Newtonian viscosity in flow. A high level of confinement is observed under physiological flow in capillaries and in the filtering organs. The shear rates experienced in vivo will therefore vary over a wide range and be complex. For example, hydrodynamic shear in partly clogged arterioles approaches 10^4 s^{-1}.[23] Indeed, others have shown that molecular confinement accelerates the deformation of entangled polymers under squeeze flow[24] in conditions comparable to blood flow. The calculated Reynolds number for individual bovine insulin molecules is Re $\sim 4 \times 10^{-4}$ and Re $\sim$ 30 for the Couette cell at the highest shear rate applied. This assumes that the buffer has a Newtonian viscosity of 1 m Pa·s and the density of water.[22] Since these values are relatively small, it is expected that insulin molecules will experience a stable (laminar) flow environment under our experimental conditions. The Couette shear exposure used in the current study is less complex than that to which the insulin is exposed in blood flow. In this sense, the present study shows the effect of the true simple shear flow on insulin conformation and aggregation. We have previously observed laminar flow in

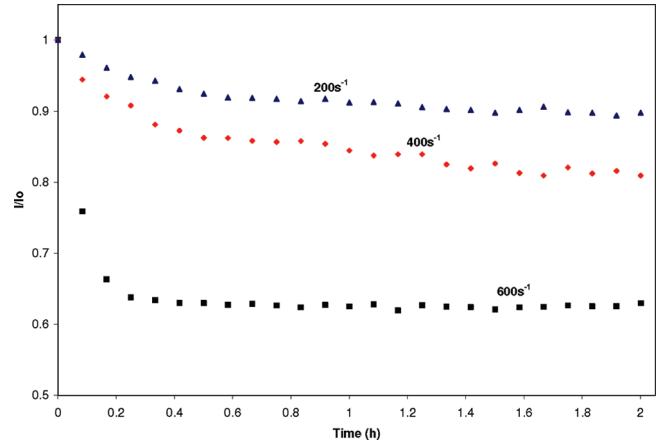

Figure 2. Shear-effect on Tyr fluorescence emission intensity of bovine insulin in flow. The emission intensity of Tyr molecules was measured for insulin samples (0.2 mg/mL) sheared at 200 (▲), 400 (♦), and 600 s^{-1} (□) over 2 h. The figure shows a time-dependent decrease in Tyr fluorescence intensity in response to flow. The flow effect is more pronounced at high shear rates. The experiments were done in 0.1% HCl (pH 1.9) with excitation/emission wavelengths of 276/305 nm.

our Couette cell at shear rates up to 1300 s^{-1}.[25] A schematic of the shear cell is shown in Figure 1 and is described elsewhere.[7] Insulin solutions were prepared by dissolving the peptide directly in 0.1% (v/v) HCl (pH 1.9) to give a concentration of ~0.2 mg/mL. The final insulin concentration was calculated from UV absorption at 280 nm, applying a molar extinction coefficient of 5.53 mM^{-1} cm^{-1}.

Figure 2 shows shear-dependent changes in the intrinsic Tyr fluorescence of bovine insulin in flow. For each curve, an initial sharp decrease in Tyr fluorescence was observed at the onset of shear. This effect was more pronounced with increasing shear rate. At shear rates of 200 and 400 s^{-1}, the intrinsic fluorescence decay approaches equilibrium after ~30 min, whereas at 600 s^{-1}, it shows complete saturation after ~15 min. The observed fluorescence decay indicates changes in the microenvironment of Tyr residues resulting from destabilization of the entire protein structure.[26] Three of the four Tyr residues in bovine insulin are located in helical segments contained in hydrophobic pockets of the protein;[11] and the emission intensity at 305 nm is an average of the parametric changes affecting the microenvironment of all Tyr residues. Therefore, the observed fluorescence decay is explained as shear-induced disruption of the helical segments of bovine insulin and subsequent exposure of hitherto sequestered Tyr residue to the aqueous environment.

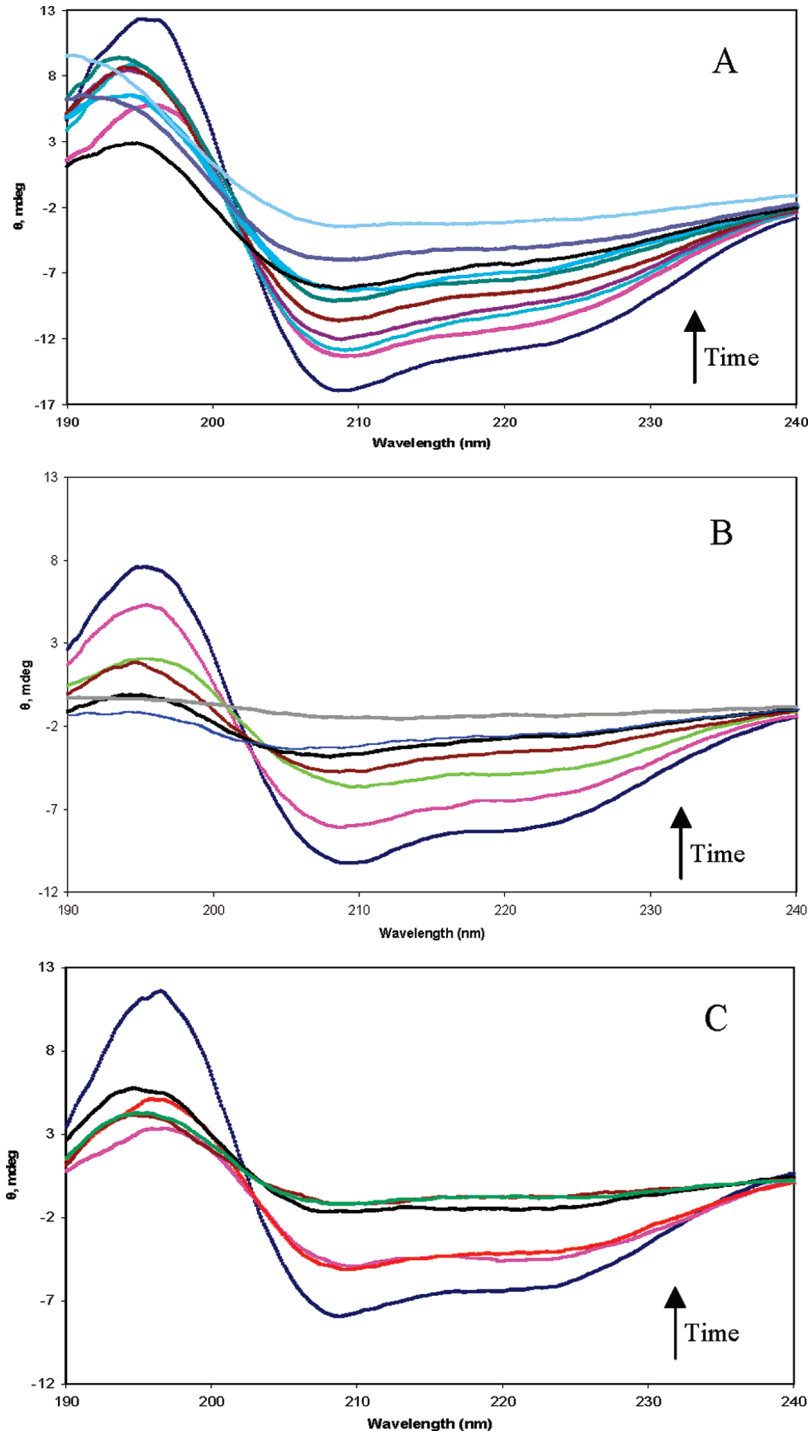

Figure 3. CD spectra showing insulin deformation in flow. The figure shows insulin samples treated at shear rates of (A) 200 s^{-1} for 0, 3, 8, 10, 13, 15, 20, 28, 33, and 40 min; (B) 400 s^{-1} for 0, 3, 5, 10, 15, 25, and 33 min; and (C) 600 s^{-1} for 0, 3, 5, 8, 20, and 30 min. The black arrows on each panel show both the direction of increasing time and decreasing negative ellipticity at $\theta_{222\ nm}$.

The rotational diffusion generated by the flow velocity facilitates effective Tyr−quencher interactions and the consequent fluorescence decay. In other words, the reduced fluorescence reflects the degree of structural disruption. This shows a relationship between the shear rates applied and the resultant structural deformation in bovine insulin.

To further probe the structural perturbation of insulin molecules in shear flow, we measured the far-UV CD spectrum of insulin solutions under Couette flow in real time. Figure 3 shows the CD spectra of insulin solutions exposed to different shear rates. At ambient temperature, the far-UV spectrum of native insulin showed two negative peak intensities at 209 and 222 nm, typical of its dominant α-helical secondary structure. At the onset of shear, this spectrum diminished in intensity; the change being more drastic with increasing shear rate. For example, at 200 s^{-1} (Figure 3, panel A) insulin retained its helical structure even after 40 min of shear although weakened in intensity, whereas at 400 and 600 s^{-1}(Figure 3, panels B and C, respectively), the helical content had diminished considerably within 15 and 8 min of shear, respectively.

The CD data was further analyzed by plotting the shear-dependent helicity change of bovine insulin as a function of time (Figure 4). We assumed a helicity of 56% for bovine insulin, similar to that of its human insulin homologue, since

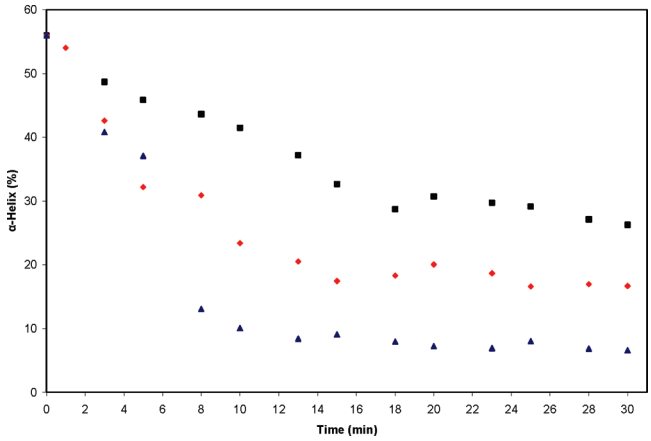

Figure 4. Shear-dependent changes in the helicity of bovine insulin in flow. The figure shows the percentage of initial α-helix remaining (change at $\theta_{222\ nm}$) as a function of time. A shear-dependent unfolding of helical segments of bovine insulin is observed, with a more pronounced effect occurring at high shear rates. Insulin samples were sheared for 200 (■), 400 (♦), and 600 s^{-1} (▲).

the sequence differences between the two are not thought to affect structural aspects or ligand binding properties of wild-type insulins.[27] The helicity of 56% indicates that ~29 of the 51 amino acid residues makeup the helical moieties of bovine insulin (i.e., 51 total residues × 0.56). We considered the initial 30 min of shear exposure because much of insulin deformation occurred within this time frame. At 200 s^{-1}, the helicity showed a gradual decrease from 56% down to 26% in the initial 30 min of shear. At 400 and 600 s^{-1}, half the helicity (56% → 28%) was lost after 9 and 6 min, respectively. The helicity decrement was obviously more drastic at 400 and 600 s^{-1} with minimums of 16.7% and 6.6%, respectively, at 30 min of shear. Therefore, out of the initial 29 helical moieties, the number remaining after the first 30 min of shear was approximately 14, 8, and 3 in the order of increasing shear rate. The absence of a lag time was obvious in the three profiles, which clearly shows that structural deformation of insulin indeed occurs at the onset of shear. It is noteworthy that the CD data further confirm the conclusions drawn from the fluorescence experiments in Figure 1.

To investigate whether insulin samples fragment under the shear rates applied, we performed SDS−PAGE analysis of pre- and post-shear insulin samples after CD measurements. Both samples gave similar bands (see the Supporting Information). This provides qualitative evidence that the primary structure of insulin monomers was maintained during shear.

Figure 5 shows AFM analysis of post-shear insulin samples obtained from Figure 1. The insulin sample sheared at 200 s^{-1} contained aggregates ranging from 3 to 50 nm in height. A sparse distribution of similar aggregates were observed in the sample treated at 400 s^{-1}. Interestingly, the sample exposed to a shear rate of 600 s^{-1} contained smaller aggregates and fibrillar forms.

Like other polymer solutions, aqueous bovine insulin exposed to simple shear flow experiences a blend of rotational and deformation velocities of equal intensity in the direction of flow.[28] In the rotational flow field, insulin molecules go through whole-body rotation, align in the direction of flow, and experience zero shear strain; hence, they maintain their native conformation. The alignment of molecules in uniform shear stress fields has previously been observed for human von Willebrand Factor[16] and a single DNA chain.[28] However, when insulin molecules cross the local plane of zero shear, the hydrodynamic drag forces in the deformation flow field trigger structural destabilization.[6] For simplicity, the deformation cycle in simple shear flow is decomposed into stretch and compressive (tumbling) events of equal magnitude. We hypothesize that helical segments unfold on extensional strain (stretching). This occurs when the drag forces in the deformation flow field overcome the intramolecular hydrogen bonds stabilizing the helical structure of native insulin. This event exposes hydrophobic regions in native insulin to the aqueous environment. As individual insulin molecules tumble end-over-end (due to rotational diffusion) in the flow field, the pressure from compression facilitates the rapid association of deformed insulin molecules, via hydrophobic and electrostatic interactions, into oligomeric aggregates. The aggregate size diminished with increasing shear rate, which shows that at high shear rates, the stress generated in the deformation cycle (specifically, the extensional flow field) breaks up aggregates that are loosely associated. This is not surprising, because the initial bonds formed between deformed protein molecules are known to be weak,[29] and an increase in shear rate boosts the frequency of stretching events in the flow field.[30] In addition, the flow velocity increases with increasing shear rate; hence, it is expected that the hydrodynamic shear stress acting on insulin monomers/aggregates would increase. The development of fibrillar aggregates at a higher shear rate (600 s^{-1}) is explained by increased polymerization of deformed bovine insulin monomers in the flow field. This is consistent with the observation that shear promotes ordering of chain elements in crystallization nucleation within a melt.[31] Indeed, empirical modeling of sheared protein solutions attribute conformational changes and accelerated aggregation to high shear rates.[32] The stability of these aggregates stems from the extensive network of hydrogen bonds between β-strands found in fibrillar forms.

We have shown a novel, real time analysis of the effect of shear on the structure and conformation of bovine insulin in a well-defined flow field. The results show that the protein experiences structural destabilization (loss in helicity) upon

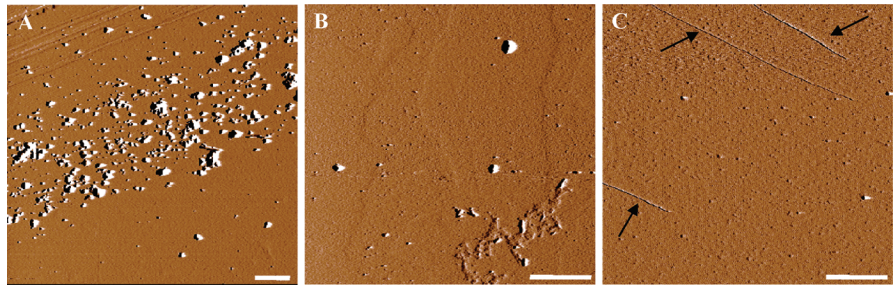

Figure 5. AFM images of insulin aggregates formed in shear flow. Images were obtained from insulin samples sheared for 2 h at (A) 200, (B) 400, and (C) 600 s^{-1}. The black arrows in panel C show fibrillar insulin aggregates. Scale bars represent 1 μm.

exposure to shear. This effect was observed at the onset of shear and was more pronounced at higher shear rates. The AFM images show the presence of large insulin aggregates at relatively low shear rates with fibrillar forms evolving at a higher shear rate. This shows that the shear stress generated at the lower shear rate (200 s^{-1}) was insufficient to break up oligomeric aggregates resulting from deformed insulin molecules. However, the deformation velocity in fast flow fields (600 s^{-1}) retarded the formation of large aggregates but, rather, promoted the ordering of deformed insulin molecules into the more stable fibrillar forms. We have previously observed the paradoxical effect of simple shear flow on protein aggregation.[18] That is, it triggers protein deformation, which is critical to fibril formation, but also inhibits the development of mature fibrils due to persistent extensional stress, which disrupts the formation of polymeric fibrillar aggregates. The present information might help explain the mechanism of shear-induced protein deformation and consequent plaque deposition in vivo.

Acknowledgment. We thank Drs. Kevin Barnham and Deborah Tew for assistance with the CD instrument. We also thank Chailean Teoh for assistance with the SDS−PAGE analysis. Funding for this project was obtained from the Australian Research Council (ARC).

Supporting Information Available: SDS-PAGE analysis of pre- and post-shear insulin samples. This material is available free of charge via the Internet at http://pubs.acs.org.

References and Notes

(1) McNally, E.; Lockwod, C. In: *Protein Formulation and Delivery*; McNally, E., Ed.; Marcel Dekker: New York, 2000; p 111.

(2) Nielsen, L.; Khurana, R.; Coats, A.; Frokjaer, S.; Brange, J.; Vyas, S.; Uversky, V. N.; Fink, A. L. *Biochemistry* **2001**, *40*, 6036.

(3) Bolder, S. G.; Sagis, L. M. C.; Venema, P.; van der Linden, E. *J. Agric. Food Chem.* **2007**, *55*, 5661.

(4) Stathopulos, P. B.; Scholz, G. A.; Hwang, Y. M.; Rumfeldt, J. A. O.; Lepock, J. R.; Meiering, E. M. *Protein Sci.* **2004**, *13*, 3017.

(5) Oliva, A.; Santoveña, A.; Fariña, J.; Llabrés, M. *J. Pharm. Biomed. Anal.* **2003**, *33*, 145.

(6) Elias, C. B.; Joshi, J. B. *Adv. Biochem. Eng. Biotechnol.* **1997**, *59*, 47.

(7) Hill, E. K.; Krebs, B.; Goodall, D. G.; Howlett, G. J.; Dunstan, D. E. *Biomacromolecules* **2006**, *7*, 10.

(8) Akkermans, C.; Venema, P.; Rogers, S. S.; van der Goot, A. J.; Boom, R. M.; van der Linden, E. *Food Biophys.* **2006**, *1*, 144.

(9) Grainger, R. J.; Ko, S.; Koslov, E.; Prokop, A.; Tanner, R. D.; Loha, V. *Appl. Biochem. Biotechnol.* **2000**, *84*, 761.

(10) Maa, Y.-F.; Hsu, C. C. *Biotechnol. Bioeng.* **1997**, *54*, 503.

(11) Whittingham, J. L.; Scott, D. J.; Chance, K.; Wilson, A.; Finch, J.; Brange, J.; Dodson, G. G. *J. Mol. Biol.* **2002**, *318*, 479.

(12) Crawford, J. G. *Med. Hypotheses* **1998**, *50*, 25.

(13) Jack, C. *Neurol. Res.* **2004**, *26*, 517.

(14) Jiang, Y.; Kohara, K.; Hiwada, K. *Association Between Risk Factors for Atherosclerosis and Mechanical Forces in Carotid Artery*; American Heart Association: Dallas, TX, 2000; Vol. 31; 2319.

(15) Howlett, G. J.; Moore, K. J. *Curr. Opin. Lipidol.* **2006**, *17*, 541.

(16) Siediecki, C. A.; Lestini, B. J.; Kottke-Marchant, K. K.; Eppell, S. J.; Wilson, D. L.; Marchant, R. E. *Blood* **1996**, *88*, 2939.

(17) Akkermans, C.; van der Goot, A. J.; Venema, P.; van der Linden, E.; Boom, R. M. *Food Hydrocolloids* **2008**, *22*, 1315.

(18) Hamilton-Brown, P.; Bekard, I.; Ducker, W. A.; Dunstan, D. E. *J. Phys. Chem. B* **2008**, *112*, 16249.

(19) Brange, J. *Galenics of insulin: the physico-chemical and pharmaceutical aspects of insulin and insulin preparations*; Springer-Verlag Berlin: Heidelberg, 1987.

(20) Brange, J.; Andersen, L.; Laursen, E. D.; Meyn, G.; Rasmussen, E. *J. Pharm. Sci.* **1997**, *86*, 517.

(21) Ehrlich, J. C.; Ratner, I. M. *Am. J. Pathol.* **1961**, *38*, 49.

(22) Stroev, P. V.; Hoskins, P. R.; Easson, W. J. *Atherosclerosis* **2007**, *191*, 276.

(23) Kroll, M. H.; Hellums, J. D.; McIntire, L. V.; Schafer, A. I.; Moake, J. L. *Blood* **1996**, *88*, 1525.

(24) Rowland, H. D.; King, W. P.; Pethica, J. B.; Cross, G. L. W. *Science* **2008**, *322*, 720.

(25) Dunstan, D. E.; Hill, E. K.; Wei, Y. *Macromolecules* **2004**, *37*, 1663.

(26) *Luminiscent Spectroscopy of Proteins*; Permyakov, E. A., Ed.; CRC Press: London, 1992, p 163.

(27) Rifkin, H.; Porte, D., Jr.; Gallon, D. *Endodontic Top.* **1992**, *2*, 139.

(28) Smith, D. E.; Babcock, H. P.; Chu, S. *Science* **1999**, *283*, 1724.

(29) Arnaudov, L. N.; de Vries, R.; Ippel, H.; van Mierlo, C. P. M. *Biomacromolecules* **2003**, *4*, 1614.

(30) Alexander-Katz, A.; Schneider, M. F.; Schneider, S. W.; Wixforth, A.; Netz, R. R. *Phys. Rev. Lett.* **2006**, *97*, 138101.

(31) Elias, H. G. *An Introduction to Plastics*; Wiley-VCH: Weinheim, 2003.

(32) Brummer, P.; Koppenol S. Protein Formulation and Delivery. In *Int. J. Pharm.*; McNally, E., Ed.; Marcel Dekker: New York, 2000; Vol. 206; pp 28.

JP903522E